PCCP

Accepted Manuscript

ROYAL SOCIETY OF CHEMISTRY

www.rsc.org/pccp

Infrared Photodissociation Spectroscopy of $M(N_2)_n^+$ (M = Y, La, Ce; n = 7-8) in the Gas Phase

Hua Xie,*,† Lei Shi,† Xiaopeng Xing,‡ Zichao Tang*,†

†State Key Laboratory of Molecular Reaction Dynamics, Dalian Institute of Chemical Physics, Chinese Academy of Sciences, Dalian 116023, China. Email: xiehua@dicp.ac.cn; zctang@dicp.ac.cn; Fax: +86-411-84675584

‡Tongji University, Department of Chemistry, 1239 Siping Road, Shanghai, 200092, China

Abstract

The $M(N_2)_n^+$ (M = Y, La, Ce; n = 7-8) complexes have been studied by infrared photodissociation (IRPD) spectroscopy and density functional theory (DFT) calculations. The experimental results indicate that the N-N stretching vibrational frequencies are red-shifted from the gas-phase N_2 value. The π back-donation is found to be a main contributor in these systems. IRPD spectra and DFT calculations reveal the coexistence of two isomers in the seven-coordinate $M(N_2)_7^+$ and eight-coordinate $M(N_2)_8^+$ complexes, respectively. The present studies on these metal-nitrogen complexes shed light on the interactions and coordinations toward N_2 with the transition and lanthanide metals.

Keywords: Metal-nitrogen complexes, Red-shifts, Lanthanide metals, Infrared photodissociation spectroscopy, Density functional theory

1. Introduction

Metal ion complexes provide important models of the chemical bonding interactions in inorganic and coordination chemistry.[1-4] The coordination number of these complexes is a topic of interest. Especially, the seven-coordinate (7C) and eight-coordinate (8C) complexes have gained a significant attention. A systematic molecular orbital analysis of IF_7, $V(CN)_7^{4-}$, $Mo(CN)_7^{5-}$ and the high-resolution powder neutron diffraction of ReF_7 have revealed the 7C structure.[5-6] Theoretical studies have predicted that $M(CO)_7$ (M=Ti, Zr, Hf) would form the 18-electron $d^{10}s^2p^6$ noble gas configuration with a stable 7C structure.[7] Gas-phase infrared photodissociation spectroscopy (IRPD) study has revealed a 7C structure for the $Nb(CO)_7^+$ and $Ta(CO)_7^+$ species but not for $V(CO)_7^+$.[8] Recent experimental and theoretical studies of $Sc(CO)_7^+$ and $Y(CO)_7^+$ have also confirmed the existence of 7C structure.[9-10] However, the six-coordinate/one-external CO (6C+1) structure has been found to be favorable in the $M(CO)_7^+$ (M=V, Ti, Zr, Hf) complexes from the IRPD measurements.[11-13] The 8C structures has been confirmed in the $M(CO)_8^+$ (M=Y, La, Ce, U) species.[9-10, 14-15] However, $Sc(CO)_8^+$ was found to consist of the seven-coordinate/one-external CO (7C+1) structure. $M(CO)_8^+$ (M= Ti, Zr, Hf) was revealed to have the six-coordinate/two-external CO (6C+2) geometry.[10, 12] Additionally, structural information is not available in the IRPD measurements of $M(CO)_7^+$ (M=Si, Mn, Co, Cu) and $M(CO)_8^+$ (M= Mn, Co, Cu).[16-19]

N_2 is an isoelectronic species compared with CO but binds more weakly to the metals, which may result in different coordination behavior. The structures and chemical bonding of metal-nitrogen complexes are of considerable interest.[20-24] The

experimental and theoretical studies have demonstrated that N_2 binds to the metals in either the "end-on" or "side-on" configurations.[25-29] Chemical reactivity of N_2 toward the metals has also been examined.[30-32] The N-N stretching vibration in the free nitrogen molecule is an IR inactive, whereas it becomes active in the metal-nitrogen ion complexes because of its dipole moment. For instance, IRPD spectra have been measured for the $M(N_2)_n^+$ (M = V, Nb; n = 7-8) complexes.[33-34] So far, much less has been done on the IRPD spectroscopy of other metal-nitrogen ion complexes as compared to the extensive metal carbonyls.

In this study, we report that the transition and lanthanide metal-nitrogen ion complexes of the form $M(N_2)_n^+$ (M = Y, La, Ce; n=7-8) are produced in a laser vaporization supersonic cluster source. IRPD spectra of these complexes are measured in the N-N stretch region. Density functional theory (DFT) calculations are carried out to aid the assignment and address the energetics and bonding mechanism. The experimental results indicate that the N-N stretch vibrations of the complexes are red-shifted compared with the free N_2 frequency value. Two isomers are confirmed to coexist in the seven-coordinate $M(N_2)_7^+$ and eight-coordinate $M(N_2)_8^+$ complexes, respectively, providing molecular understanding of the bonding of N_2 to the early lanthanide metals.

2. Experimental method

IRPD experiments were carried out using a home-made apparatus that included a laser vaporization supersonic cluster source and a tandem time-of-flight (TOF) mass spectrometer. The experimental setup has been previously described in detail.[15]

Briefly, a 532 nm laser beam from the Nd: YAG laser was focused to vaporize the rotating metal targets. Purities of the targets were higher than 99.9%. The $M(N_2)_n^+$ complexes were produced by the reactions of the vaporized species with pure N_2. The N_2 purity was higher than 99.9%. The stagnation pressure of N_2 was approximately 7-10 atm. N_2 was introduced into the vacuum region using a pulsed valve. After the free expansion, all products were skimmed into the acceleration region and the cationic complexes were analyzed using the first stage of the TOF system. Then, the cations of interest were mass selected and decelerated into the extraction region of a vertical second stage of the TOF system. There, the selected cations were dissociated by a tunable pulsed infrared photodissociation laser. The dissociation fragments and the remaining parent cations were analyzed using the vertical second stage of the TOF mass spectrometer. The infrared spectra were obtained by recording the yield of the fragment cations as a function of the IR laser wavelength. Typical spectra were recorded by scanning the infrared laser with a 2 cm^{-1} step. Additionally, approximately 300 laser shots were averaged for each wavelength.

The tunable infrared laser beam was generated using a KTP/KTA optical parametric oscillator/amplifier system (OPO/OPA, Laser Vision) that was pumped by a Continuum Surelite Nd:YAG laser. This system was tunable from 2000 to 5000 cm^{-1} with a line width of approximately 1 cm^{-1}. The infrared laser beam was loosely focused using a CaF_2 convex lens before entering the infrared photodissociation region. The wavelength of the OPO laser output was calibrated using a commercial wavelength meter (Bristol, 821 Pulse Laser Wavelength Meter).

3. Computational methods

The DFT calculations were performed to study the structures and bonding of $M(N_2)_n^+$ (M=Y, La, Ce; n=7-8). Their lowest or the second lowest spin states were considered. The structures were optimized using the B3LYP method with the LANL2DZ basis sets for all elements.[35-36] The optimizations for each species started from several geometries that covered all reasonable chemically bonded structures. The obtained minima were further optimized using the B3LYP and BP86 methods,[37] in which the 6-311+G (3df) basis sets was used for N and the SDD (SC-RECP, MWB28) basis set for Y, La and Ce.[38] The frequency analysis was applied to make sure that all of the obtained structures were the real minima. The harmonic vibrational frequencies were calculated with the analytic second derivatives that were based on the results from the B3LYP/6-311G (3df) & SDD levels and were scaled by a factor of 0.972, which was determined by computing the average value that was needed to make the calculated and experimental vibrational frequencies match for the $M(N_2)_n^+$ cluster cations. IR stick spectra were convoluted by a Gaussian line shape function with a full width at half-maximum (FWHM) of 10 cm^{-1}. All calculations were performed using a Gaussian 09 program.[39]

4. Results and discussion

Laser vaporization of the metal rods in pure N_2 produces the metal complexes of $M(N_2)_n^+$ (M=Y, La, Ce; n=7-8). Pure N_2 molecules react very fast with the metal species, thus, preventing them from generating large metal cationic clusters under our experimental conditions. The complexes containing larger coordination number could

hardly be detected due to the hot cluster source in the experiments. These metal species of interest are mass-selected and reach the infrared photodissociation region. The selected cations can absorb the photons and produce fragmentation by losing N_2(s) when the IR-active vibration of the cation is resonant with the tunable infrared laser frequency.

4.1 Experimental IRPD spectra of $M(N_2)_n^+$ (M=Y, La, Ce; n=7-8)

Fig. 1 shows the experimental IRPD spectra of $M(N_2)_8^+$ (M = Y, La, Ce) in the N-N stretching region. The dissociation experimental results of these cationic species indicate that they have a single band. The N-N stretching vibrational frequencies of these cations for Y, La and Ce are observed at 2226, 2260, and 2260 cm^{-1}, respectively, which are red-shifted from the free N_2 frequency value (2330 cm^{-1}). $Y(N_2)_8^+$ exhibits a larger red-shift than the $La(N_2)_8^+$ and $Ce(N_2)_8^+$ species. These $M(N_2)_8^+$ species dissociate by losing one N_2 molecule with a high efficiency under the focused infrared laser beam. The $Y(N_2)_8^+$ can be depleted by approximately 27% when the infrared laser energy is approximately 10 mJ/pulse/cm^2. The spatial overlap of the focused laser with the ion beam in the experiments is 3 millimeters. The $La(N_2)_8^+$ and $Ce(N_2)_8^+$ can be depleted approximately 11% and 16% with the same laser energy of the $Y(N_2)_8^+$ cation, respectively. The observed infrared photodissociation spectra of the $M(N_2)_8^+$ (M=Y, La, Ce) are more than 70 cm^{-1} red-shifted from the position of the free N_2 molecule. Each of the spectra has only one clear band, and this observation is similar to the previously reported spectra of the $M(CO)_8^+$ (M=Y, La, Ce, U) complexes.[10, 14-15]

The experimental IRPD spectra of $M(N_2)_7^+$ (M=Y, La, Ce) in the N-N stretching region are displayed in Fig. 2. Their experimental results show two broad bands. They also have the N-N stretching vibrations that are red-shifted from the free N_2 frequency value. These $M(N_2)_7^+$ complexes are observed to dissociate by losing one N_2 molecule with a low efficiency under the focused infrared laser beam. The higher peaks of these $M(N_2)_7^+$ complexes can be depleted by approximately 3% when the infrared laser energy is approximately 10 mJ/pulse/cm^2. The intensity ratios of the two peaks are approximately 1:6, 1:4 and 1:3, respectively. The observed IRPD of the $M(N_2)_7^+$ (M=Y, La, Ce) also have more than a 70 cm^{-1} red-shift from the position of the free N_2 molecule.

4.2 Optimized structures

Optimized structures of the low-lying isomers of $M(N_2)_n^+$ (M=Y, La, Ce; n=7-8) are shown in Fig. 3. Their geometries and electronic states are also indicated. Table 1 displays relative energies of $M(N_2)_{7,8}^+$ (M = Y, La, Ce) and the lowest binding energies for the loss of one N_2 in $M(N_2)_8^+$ (M = Y, La, Ce).

The lowest energy structures (labeled iso A in Fig. 3) for $M(N_2)_8^+$ (M = Y, La) are predicted to have an O_h geometry with the $^3A_{1g}$ state, in which eight N_2 ligands are equally bound to the central Y or La atom. Next energetically higher isomer (iso B) consists of the D_{4d} structure with the $^1A_1$ state. These findings are reminiscent of the O_h and D_{4d} structures for $M(CO)_8^+$ (M =Y, La, U) complexes.[9-10, 14] For $Ce(N_2)_8^+$, the lowest energy structure is calculated to have a quartet state ($^4A_{2u}$) and a D_{4h} geometry, slightly distorted from the O_h geometry. Iso B has the C_1 structure with the ^{2}A state,

which lies slightly higher in energy than iso A (Table 1 and Fig. 3).

For $M(N_2)_7^+$ (M = Y, La), the C_{3v} geometry with the $^3A_1$ state is the lowest energy structure (iso A), which could be viewed as a capped octahedron. Analogous C_{3v} structures have been predicted for the $M(CO)_7^+$ (M = Nb, Ta, Sc, Y, La) species.[8-10] The lowest energy structure for $Ce(N_2)_7^+$ consists of the C_s geometry with the $^4A'$ state (iso A), which is slightly distorted from the C_{3v} structure that is predicted for $M(N_2)_7^+$ (M = Y, La). Note that theoretical calculations for these two structures always contain some spin contaminations. For instance, the eigenvalue of the S^2 operator in the calculation of the doublet $Ce(N_2)_7^+$ is approximately 1.75, which is much higher than the expected 0.75 value for the doublet species. Such deviation indicates a significant state mixing with the higher spin states. Additionally, the theoretical relative energy and the bond energy for the doublet state are always higher in energy than the quartet state (Table 1).

4.3 Comparisons of the experimental IRPD spectra with simulated ones

The analysis of the dissociation ratio for $M(N_2)_8^+$ reveals that it is always greater than 11%. Therefore, this indicates the high dissociation probabilities in these systems. However, the low dissociation probabilities of $M(N_2)_7^+$ are observed in the experiments. At the B3LYP/6-311G (3df) & SDD level, the lowest binding energies for the loss of one N_2 in $M(N_2)_8^+$ (M = Y, La, Ce) (Table 1) indicate that assuming internally cold complexes, the absorption of one photon around 2300 cm^{-1} is required to overcome the dissociation limit, except for iso B of $Ce(N_2)_8^+$.

Comparison of the experimental to simulated infrared spectra of the $M(N_2)_n^+$ (M

= Y, La, Ce; *n*=7-8) complexes is shown in Figs. 4 and 5. Table 2 displays the representative frequencies of these cations calculated from the B3LYP method. For $Y(N_2)_8^+$, the simulated N-N stretching vibrational frequencies in the isomers A and B are located at 2251 and 2245 cm^{-1}, respectively, which agree with the experimental values. Calculated band positions for $La(N_2)_8^+$ and $Ce(N_2)_8^+$ also reproduce the experiments. As illustrated in Figs. S1-S3 (see ESI), the simulated N-N stretching vibrational frequencies in the (6C+2) and (7C+1) structures of $M(N_2)_8^+$ (*M* =Y, La) and (7C+1) structure of $Ce(N_2)_8^+$ are obviously different from the experiments. Note that the optimization of (6C+2) structure for $Ce(N_2)_8^+$ is very hard to be converged because of the extremely flat potential surface. These comparisons between theoretical and experimental results lead to the conclusion that the eight-coordinate (8C) structures dominate for the $M(N_2)_8^+$ (M=Y, La, Ce) in gas phase, and the corresponding two configurations with the triplet O_h geometry and the singlet D_{4d} geometry are not distinguishable under the current experimental conditions.

For $Ce(N_2)_7^+$, one peak of N-N stretching vibrational mode is observed at 2250 cm^{-1} in the most stable structure of iso A, whereas two peaks at 2222 and 2261 cm^{-1} with the intensity ratio of approximate 1:1 in isomer B (Fig. 5). Experimentally, the ratio of two peaks at 2228 and 2252 cm^{-1} is about 1:3, implying the coexistence of isomers A and B and the population of iso A should be higher than iso B. Similar results have been obtained for $Y(N_2)_7^+$ and $La(N_2)_7^+$ (Fig. 5), respectively.

The experimental N-N stretching vibrational frequencies in $M(N_2)_n^+$ (*M*=Y, La, Ce; *n*=7-8) show red-shifted features from that of free N_2. This is similar to the

$M(CO)_8^+$ (M=Y, La, Ce) recently reported.[10, 15] Experimental C-O/N-N stretching vibrational frequencies of the $M(CO)_8^+$ and $M(N_2)_8^+$ (*M* = Y, La, Ce) cations and their shifts with respect to free CO/N_2 molecules are compared in Table S1. According to the Dewar-Chatt-Duncanson model, this red-shifted phenomenon is attributed to the π-type back-donation.[1, 14] The red-shifts of C-O stretching vibrational frequencies in $M(CO)_8^+$ (*M*=Y, La, Ce) are 56, 33, and 35 cm^{-1} with respect to the free carbon monoxide (2143 cm^{-1}) (Table S1),[10, 15] which are smaller than those of N-N stretching vibrational frequencies in $M(N_2)_8^+$ (*M*=Y, La, Ce) are 104, 70, and 70 cm^{-1} with respect to the free N_2 (2330 cm^{-1}). This suggests that the $M(N_2)_8^+$ complexes have more contributions from the π back-donation in these cations than the corresponding carbonyl cations. The calculated C-O/N-N bond lengths in the metal complexes are elongated as compared to the free CO/N_2 molecules. As given in Table S1, the deviations of fuzzy bond order of the CO moieties in $M(CO)_8^+$ (*M* = Y, La, Ce) are calculated to be about -0.16, -0.14 and -0.14, respectively, which are smaller than those for the N_2 moieties in $M(N_2)_8^+$ (-0.37 for Y, -0.31 for La and -0.24 for Ce), consequently, resulting in less activation of CO by these metals. This supports the experimental observations of the red-shifts of C-O/N-N stretching vibrational frequencies. In the previous studies, the $Y(CO)_8^+$ was predicted to be an eight-coordination (8C) structure and it was rationalized using the 18-electron $d^{10}s^2p^6$ configuration. In this work, the $Y(N_2)_8^+$ is also a similar 18-electron rule complex. The $La(N_2)_8^+$ and $Ce(N_2)_8^+$ complexes cannot be rationalized via the 18-electron rules, even if their *f* orbital is not taken into consideration.

Until recently, the eight-coordination (8C) structure has been identified in the metal carbonyls $M(CO)_8^+$ (M=Y, La, Ce, U) cations,[9-10, 14-15] as well as seven-coordination (7C) structure in the $M(CO)_7$ (M=Ti, Zr, Hf) and $M(CO)_7^+$ (M=Nb, Ta, Sc, Y, La) systems.[8-10, 12] In the present studies of the metal-nitrogen complexes, the 8C and 7C structures have been fortunately confirmed in the $M(N_2)_8^+$ and $M(N_2)_7^+$ (M=Y, La, Ce; n=7-8) complexes, respectively, implying that the formation of the metal-nitrogen and carbonyl complexes with such high coordination number could be a common feature for Y, La and Ce.

5. Conclusions

The $M(N_2)_n^+$ (M=Y, La, Ce; n=7-8) complexes have been produced and analyzed using a laser vaporization supersonic cluster source and a tandem time-of-flight (TOF) mass spectrometer. These cluster cations have been studied via the infrared photodissociation spectroscopy and theoretical calculations in the N-N stretching region. The experimental results indicate that the N-N stretching vibrational frequencies of the complexes are red-shifted with respect to the free N_2, which are larger than the red-shifts of C-O stretching vibrational frequencies in the corresponding carbonyls $M(CO)_8^+$. This indicates that the N_2 molecules gain more activation by these metals than CO, which is supported by the calculated fuzzy bond order of the CO/N_2 moieties. IRPD spectra and DFT calculations reveal the coexistence of two isomers in the seven-coordinate $M(N_2)_7^+$ and eight-coordinate $M(N_2)_8^+$ complexes, respectively, implying that the formation of the metal-nitrogen and carbonyl complexes with such high coordination number could be a common

feature for Y, La and Ce.

Supporting Information

B3LYP simulated C-O/N-N bond lengths, fuzzy bond order of the CO/N_2 moieties, and experimental C-O/N-N stretching vibrational frequencies of the $M(CO)_8^+$ and $M(N_2)_8^+$ (M = La, Ce) cations and their shifts with respect to free CO/N_2 molecules (Table S1), Comparison of experimental IRPD spectrum with B3LYP simulated ones of (6C+2) and (7C+1) structures of $M(N_2)_8^+$ (M=Y, La) and (7C+1) structure of $Ce(N_2)_8^+$ (Figs. S1-S3). This material is available free of charge via the Internet at http://pubs.rsc.org.

Acknowledgments

This work was supported by the National Natural Science Foundation of China (Grant No. 21273233, 21273278, 21503222), the Ministry of Science and Technology of China (Grant No. 2011YQ09000505), and the Chinese Academy of Sciences. We thank Prof. Ling Jiang for his support in the tunable infrared laser system and fruitful discussions.

Notes and references

1 J. E. Huheey, E. A. Keiter and R. L. Keiter, *Inorganic Chemistry Principles of Structure and Reactivity*. Harper Collins: New York: 1993.

2 F. A. Cotton, G. Wilkinson, C. A. Murillo and M. Bochmann, *Advanced inorganic chemistry*. 6th ed. ed.; John Wiley & Sons: New York: 1999.

3 G. Frenking and N. Fröhlich, The Nature of the Bonding in Transition-Metal Compounds. *Chem. Rev.*, 2000, **100**, 717.

4 M. F. Zhou, L. Andrews and C. W. Bauschlicher, Spectroscopic and Theoretical Investigations of Vibrational Frequencies in Binary Unsaturated Transition-Metal Carbonyl Cations, Neutrals, and Anions. *Chem. Rev.*, 2001, **101**, 1931.

5 R. Hoffmann, B. F. Beier, E. L. Muetterties and A. R. Rossi, Seven-coordination. A molecular orbital exploration of structure, stereochemistry, and reaction dynamics. *Inorg. Chem.*, 1977, **16**, 511.

6 T. Vogt, A. N. Fitch and J. K. Cockroft, Crystal and Molecular Structures of Rhenium Heptafluoride. *Science*, 1994, **263**, 1265.

7 Q. Luo, Q. S. Li, Z. H. Yu, Y. Xie, R. B. King and H. F. Schaefer, Bonding of Seven Carbonyl Groups to a Single Metal Atom: Theoretical Study of $M(CO)_n$ (M = Ti, Zr, Hf; n = 7, 6, 5, 4). *J. Am. Chem. Soc.*, 2008, **130**, 7756.

8 A. M. Ricks, Z. D. Reed and M. A. Duncan, Seven-Coordinate Homoleptic Metal Carbonyls in the Gas Phase. *J. Am. Chem. Soc.*, 2009, **131**, 9176.

9 X. P. Xing, J. Wang, H. Xie, Z. L. Liu, Z. B. Qin, L. J. Zhao and Z. C. Tang, Octacoordinate metal carbonyls of scandium and yttrium: theoretical calculations and experimental observation. *Rapid Commun. Mass Spectrom.*, 2013, **27**, 1403.

10 A. D. Brathwaite, J. A. Maner and M. A. Duncan, Testing the Limits of the 18-Electron Rule: The Gas-Phase Carbonyls of Sc^+ and Y^+. *Inorg. Chem.*, 2014, **53**, 1166.

11 A. M. Ricks, A. D. Brathwaite and M. A. Duncan, Coordination and Spin States in Vanadium Carbonyl Complexes ($V(CO)_n^+$, n = 1–7) Revealed with IR Spectroscopy. *J. Phys. Chem. A*, 2013, **117**, 1001.

12 A. D. Brathwaite and M. A. Duncan, Infrared Photodissociation Spectroscopy of Saturated Group IV (Ti, Zr, Hf) Metal Carbonyl Cations. *J. Phys. Chem. A*, 2013, **117**, 11695.

13 X. Zhou, J. Cui, Z. H. Li, G. Wang, Z. Liu and M. F. Zhou, Carbonyl Bonding on Oxophilic Metal Centers: Infrared Photodissociation Spectroscopy of Mononuclear and Dinuclear Titanium Carbonyl Cation Complexes. *J. Phys. Chem. A*, 2013, **117**, 1514.

14 A. M. Ricks, L. Gagliardi and M. A. Duncan, Infrared Spectroscopy of Extreme Coordination: The Carbonyls of U^+ and UO_2^+. *J. Am. Chem. Soc.*, 2010, **132**, 15905.

15 H. Xie, J. Wang, Z. B. Qin, L. Shi, Z. C. Tang and X. P. Xing, Octacoordinate Metal Carbonyls of Lanthanum and Cerium: Experimental Observation and Theoretical Calculation. *J. Phys. Chem. A*, 2014, **118**, 9380.

16 A. M. Ricks, J. M. Bakker, G. E. Douberly and M. A. Duncan, Infrared Spectroscopy and Structures of Cobalt Carbonyl Cations, $Co(CO)_n^+$ (n = 1−9). *J. Phys. Chem. A*, 2009, **113**, 4701.

17 Z. D. Reed and M. A. Duncan, Infrared Spectroscopy and Structures of Manganese Carbonyl Cations, $Mn(CO)_n^+$ (n = 1–9). *J. Am. Soc. Mass. Spectrom.*, 2010, **21**, 739.

18 A. D. Brathwaite, Z. D. Reed and M. A. Duncan, Infrared Photodissociation Spectroscopy of Copper Carbonyl Cations. *J. Phys. Chem. A*, 2011, **115**, 10461.

19 A. D. Brathwaite and M. A. Duncan, Infrared Spectroscopy of $Si(CO)_n^+$ Complexes: Evidence for Asymmetric Coordination. *J. Phys. Chem. A*, 2012, **116**, 1375.

20 Chatt, J. The reactions of dinitrogen in its mononuclear complexes. *J. Organomet. Chem.*, 1975, **100**, 17.

21 J. Chatt and R. L. Richards, The reactions of dinitrogen in its metal complexes. *J. Organomet. Chem.*, 1982, **239**, 65.

22 K. Eller and H. Schwarz, Organometallic chemistry in the gas phase. *Chem. Rev.*, 1991, **91**, 1121.

23 F. A. Khan, D. L. Steele and P. B. Armentrout, Ligand Effects in Organometallic

Thermochemistry: The Sequential Bond Energies of $Ni(CO)_x^+$ and $Ni(N_2)_x^+$ (x = 1-4) and $Ni(NO)_x^+$ (x = 1-3). *J. Phys. Chem.*, 1995, **99**, 7819.

24 B. L. Tjelta, D. Walter and P. B. Armentrout, Determination of weak Fe^+–L bond energies (L = Ar, Kr, Xe, N_2, and CO_2) by ligand exchange reactions and collision-induced dissociation. *Int. J. Mass Spectrom.*, 2001, **204**, 7.

25 C. W. Bauschlicher, L. G. M. Pettersson and P. E. M. Siegbahn, The bonding in FeN_2, FeCO, and Fe_2N_2: Model systems for side-on bonding of CO and N_2. *J. Chem. Phys.*, 1987, **87**, 2129.

26 R. L. Asher, D. Bellert, T. Buthelezi and P. J. Brucat, Optical Excitation of $Co^+.N_2$. *J. Phys. Chem.*, 1995, **99**, 1068.

27 C. Heinemann, J. Schwarz and H. Schwarz, Ground State of $Co(N_2)^+$. *J. Phys. Chem.*, 1996, **100**, 6088.

28 A. Zacarías, H. Torrens and M. Castro, A density functional study of Fe-N_2, Fe-N_2^+, and Fe-N_2. *Int. J. Quantum Chem.*, 1997, **61**, 467.

29 H. A. Duarte, D. R. Salahub, T. Haslett and M. Moskovits, $Fe(N_2)_n$ (n = 1−5): Structure, Bonding, and Vibrations from Density Functional Theory. *Inorg. Chem.*, 1999, **38**, 3895.

30 A. Bérces, P. A. Hackett, L. Lian, S. A. Mitchell and D. M. Rayner, Reactivity of niobium clusters with nitrogen and deuterium. *J. Chem. Phys.*, 1998, **108**, 5476.

31 Y. D. Kim and G. Ganteför, Non-dissociative adsorption of diatomic molecules on nanoclusters at room temperature. *Chem. Phys. Lett.*, 2003, **382**, 644.

32 Y. D. Kim and G. Ganteför, Formation of activated diatomic species on mass-selected clusters. *J. Mol. Struct.*, 2004, **692**, 139.

33 E. D. Pillai, T. D. Jaeger and M. A. Duncan, IR Spectroscopy and Density Functional Theory of Small $V^+(N_2)_n$ Complexes. *J. Phys. Chem. A*, 2005, **109**, 3521.

34 E. D. Pillai, T. D. Jaeger and M. A. Duncan, IR Spectroscopy of $Nb^+(N_2)_n$ Complexes: Coordination, Structures, and Spin States. *J. Am. Chem. Soc.*, 2007, **129**, 2297.

35 P. J. Hay and W. R. Wadt, Ab initio effective core potentials for molecular calculations. Potentials for K to Au including the outermost core orbitals. *J. Chem.*

Phys., 1985, **82**, 299.

36 A. D. Becke, Density□functional thermochemistry. III. The role of exact exchange. *J. Chem. Phys.*, 1993, **98**, 5648.

37 A. D. Becke, Density-functional exchange-energy approximation with correct asymptotic behavior. *Phys. Rev. A*, 1988, **38**, 3098.

38 M. Dolg, H. Stoll and H. Preuss, Energy-adjusted abinitio pseudopotentials for the rare earth elements. *J. Chem. Phys.*, 1989, **90**, 1730.

39 M. J. Frisch, G. W. Trucks, H. B. Schlegel, G. E. Scuseria, M. A. Robb, J. R. Cheeseman, G. Scalmani, V. Barone, B. Mennucci and G. A. Petersson et. al. Gaussian 09, Revision A02, Gaussian, Inc., Wallingford, CT. 2009.

Table 1. Relative energies (kcal/mol) of $M(N_2)_{7,8}^+$ (M = Y, La, Ce) and the lowest binding energies (kcal/mol) for the loss of one N_2 in $M(N_2)_8^+$ (M = Y, La, Ce)

Complex	Spin State	Relative Energy		Binding Energy	
		B3LYP	BP86	B3LYP	BP86
$Y(N_2)_8^+$	Singlet	4.2	3.8	5.6	7.1
	Triplet	0.0	0.0	3.9	4.9
$Y(N_2)_7^+$	Singlet	6.0	6.0		
	Triplet	0.0	0.0		
$La(N_2)_8^+$	Singlet	6.0	6.1	6.2	7.0
	Triplet	0.0	0.0	6.3	7.2
$La(N_2)_7^+$	Singlet	6.0	5.8		
	Triplet	0.0	0.0		
$Ce(N_2)_8^+$	Doublet	2.2	2.3	8.4	5.6
	Quartet	0.0	0.0	5.2	5.0
$Ce(N_2)_7^+$	Doublet	5.4	2.8		
	Quartet	0.0	0.0		

Table 2. Scaled N-N stretching vibrational frequencies (cm^{-1}) and their intensities in $Y(N_2)_{7,8}^+$, $La(N_2)_{7,8}^+$ and $Ce(N_2)_{7,8}^+$ calculated from the B3LYP method.

Complex	Spin	freq (intensities)
$Y(N_2)_8^+$	Singlet	2245(1310), 2245(1310), 2246(1217)
	Triplet	2252(1245), 2252(1245), 2252(1245)
$Y(N_2)_7^+$	Singlet	2203(290),2207(329),2225(181),2232(1388), 2238(914),2241(709),2298(14)
	Triplet	2218(112),2218(112),2221(319), 2229(1348),2229(1348),2242(920)
$La(N_2)_8^+$	Singlet	2254(1327),2254(1327),2257(1306)
	Triplet	2262(1281), 2262(1281), 2262(1281)
$La(N_2)_7^+$	Singlet	2221(339),2223(327),2233(329),2240(1358), 2248(988),2251(590),2296(28)
	Triplet	2240(56),2240(56),2240(8), 2247(1113),2249(1353),2249(1353)
$Ce(N_2)_8^+$	Doublet	2259(1311),2259(1313),2262(1130)
	Quartet	2258(1423),2258(1423),2264(1133)
$Ce(N_2)_7^+$	Doublet	2217(322),2219(833),2230(851), 2253(108),2260(766),2264(1032)
	Quartet	2236(94),2240(379),2241(372), 2246(921),2252(1181),2253(1017)

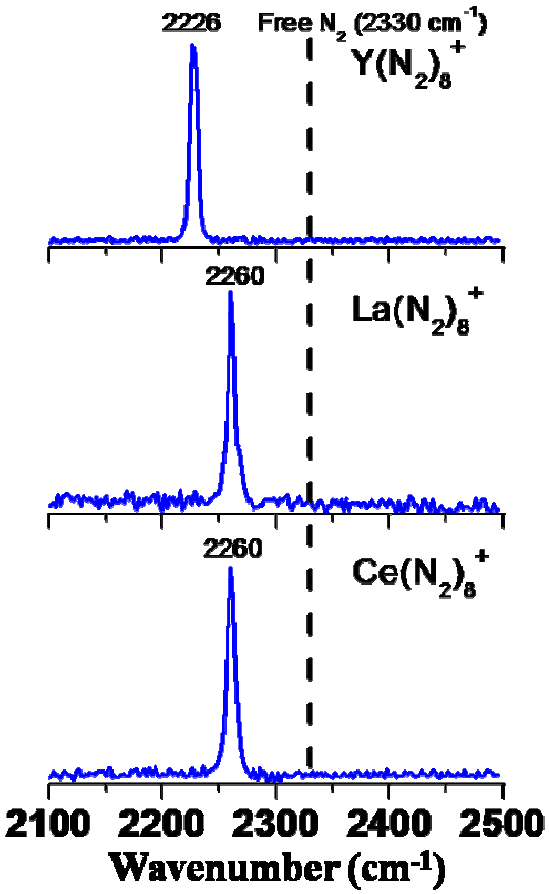

Fig. 1. Experimental infrared photodissociation spectra of $M(N_2)_8^+$ (M = Y, La, Ce) in the N-N stretching region.

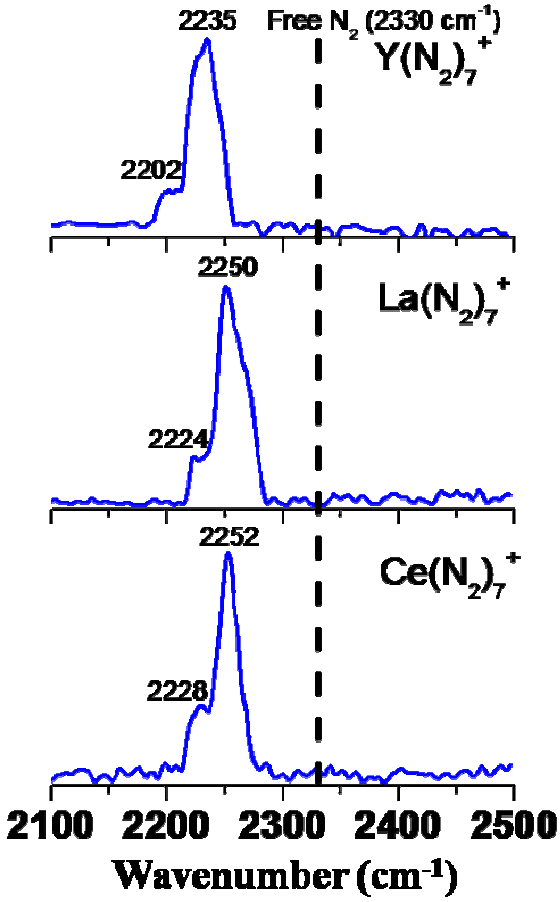

Fig. 2. Experimental infrared photodissociation spectra of $M(N_2)_7^+$ (M = Y, La, Ce) in the N-N stretching region.

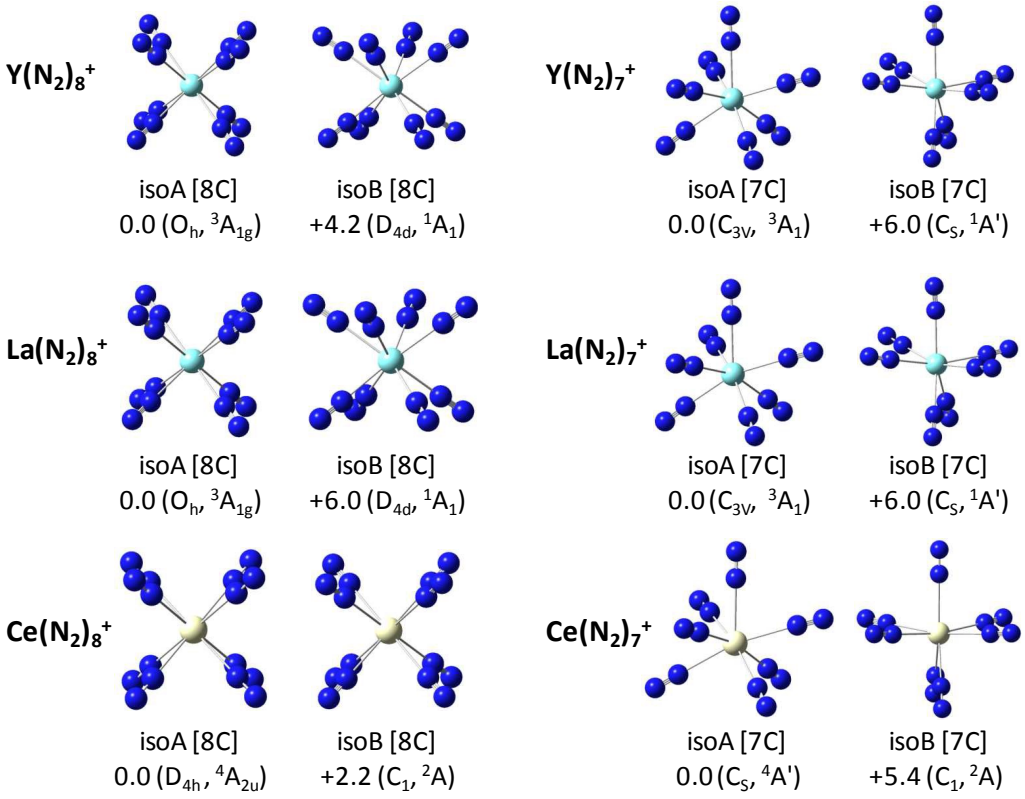

Fig. 3. Optimized structures of the low-energy isomers of $M(N_2)_n^+$ (M = Y, La, Ce; n=7-8). The pattern with coordination number is given inside square brackets. B3LYP relative energies are listed in kcal/mol and the symmetries and electronic states are indicated inside the parenthesis.

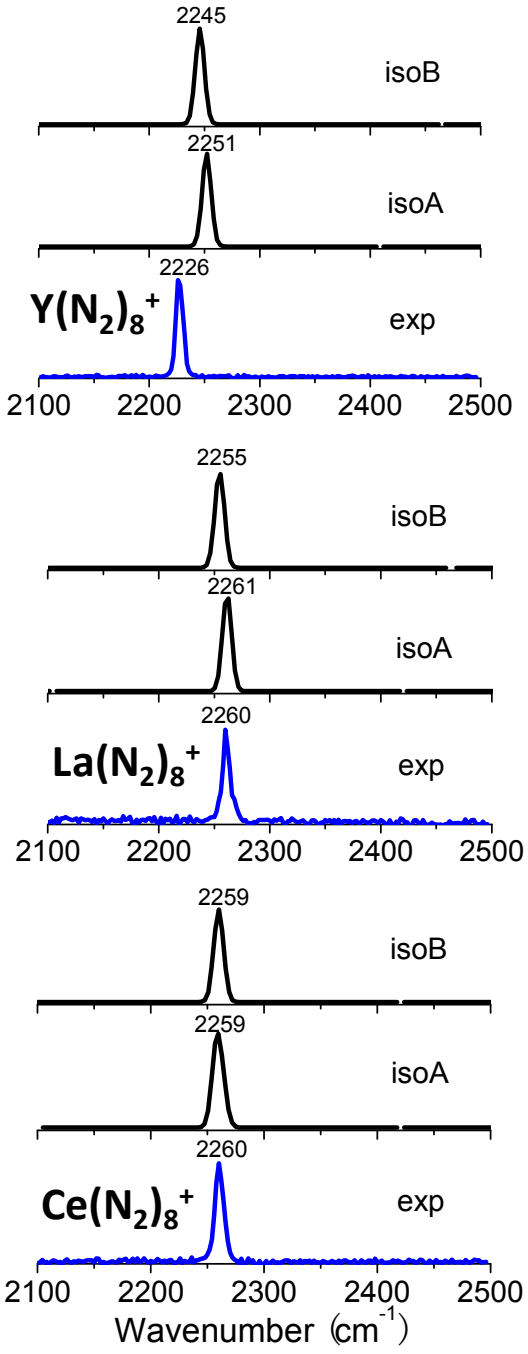

Fig. 4. Experimental (in blue) and B3LYP simulated (in black) infrared photodissociation spectra of $M(N_2)_8^+$ (M = Y, La, Ce).

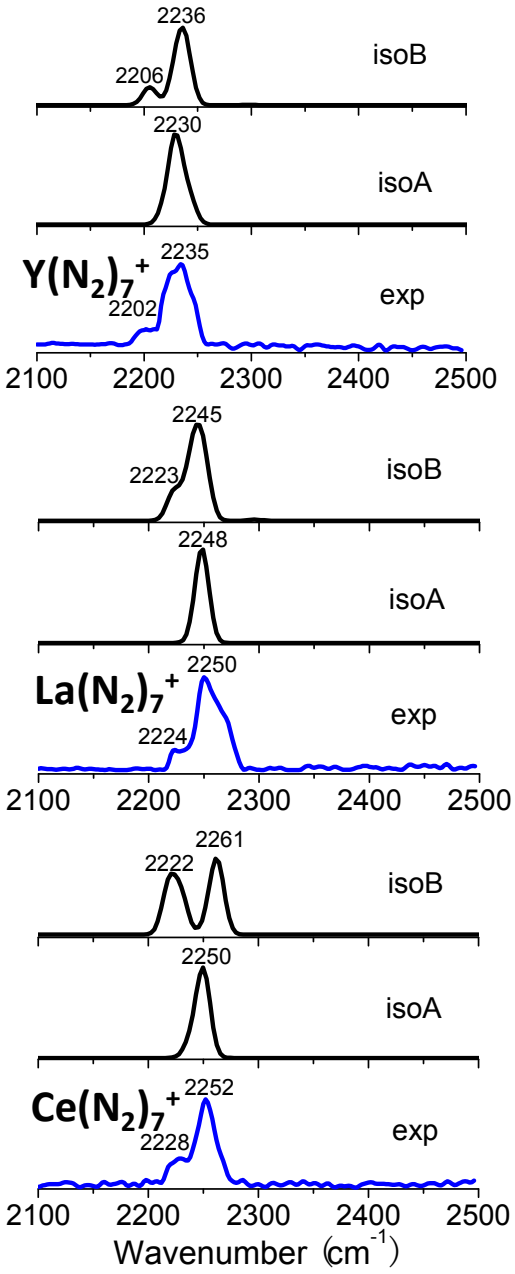

Fig. 5. Experimental (in blue) and B3LYP simulated (in black) infrared photodissociation spectra of $M(N_2)_7^+$ (M = Y, La, Ce).